Electronic properties of the Penrose lattice. I. Energy spectrum and wave functions

Hirokazu Tsunetsugu
Institute for Solid State Physics, University of Tokyo, Tokyo 106, Japan

Takeo Fujiwara
Department of Applied Physics, University of Tokyo, Tokyo 113, Japan

Kazuo Ueda
Institute of Materials Science, University of Tsukuba, Tsukuba, Ibaraki, Japan

Tetsuji Tokihiro
Department of Physics, University of Pennsylvania, Philadelphia, Pennsylvania 19104
and Department of Applied Physics, University of Tokyo, Tokyo 113, Japan
(Received 21 June 1990)

The electronic structure of the two-dimensional Penrose lattice is studied by numerical diagonalization of a tight-binding Hamiltonian for finite systems with up to 3571 sites. We have analyzed the smoothness of the energy spectrum and localization behavior of the wave functions by level statistics and a generalized participation ratio. The results show that the energy spectrum contains a singular part, and most of the wave functions are critical, i.e., neither extended nor localized. These behaviors of the electronic properties are discussed based on their quasiperiodic lattice structure.

I. INTRODUCTION

The observation of sharp diffraction spots with icosahedral symmetry in a rapidly quenched Al-Mn alloy by Shechtman *et al.*[1] called into question our long-standing belief that every ordered structure must be periodic. It clearly indicated the existence of long-range order without translational symmetry. The notion of crystals was generalized independently by Levine and Steinhardt[2] on the structures which are not periodic but still hold a kind of translational long-range order, called *quasiperiodicity*. They classified materials with these structural properties into a new class of ordered structures and called them quasicrystals (QC).[3] Actually, they showed that the structure factor of a three-dimensional (3D) generalization of the Penrose lattice was close to the observed icosahedral diffraction pattern of the Al-Mn alloy. Since the first discovery, many materials have been found to have quasiperiodicity[4] and some of them show 2D quasiperiodic structures with decagonal, octagonal, or dodecagonal symmetries.[5] Now it is known that the QC phase is not only metastable but thermodynamically stable in some materials such as Al-Li-Cu alloys.[6] Therefore QC are not rare variations of usual crystals, but rather they constitute a new category of condensed matter comparable to the conventional categories—crystals and disordered materials (amorphous).

The structure of QC has a character intermediate between crystals and disordered materials: e.g., the lack of translational symmetry is common with disordered materials, but the sharp diffraction spots are common with crystals. It is well known that disorder in the lattice structure brings qualitative change to electronic properties when strength of the disorder exceeds a critical value, and wave functions, in particular, always become localized in 1D and 2D disordered materials, i.e., the critical strength is zero, which is called the Anderson localization.[7] We hence expect that due to the nonperiodic lattice structure, the electronic properties of QC show behaviors intermediate between crystals and disordered materials or possibly specific to the quasiperiodicity. Alternatively, we hope that this study may throw new light on the localization mechanism in amorphous materials from the viewpoint of structural disorder.

Some interesting electronic properties have actually been found in a 1D quasicrystal, the Fibonacci chains (FC)—the model where the perturbations such as on-site potentials (or transfer energies) are quasiperiodically arranged in the space following the Fibonacci sequence.[8] The most interesting property is the energy spectrum with a self-similar structure of energy gaps, called "the devil's staircase," and the total bandwidth decreases down to zero in a power law with increasing system size $B \sim N^{-\alpha}$. It is mathematically proved that the energy spectrum is a Cantor set and singular continuous.[9] Another important consequence that came out of the study is the belief that all the eigenstates are critical,[10] i.e., neither extended all over the lattice as are the Bloch states, nor exponentially localized as are the strongly localized states of the Anderson localization. However, a recent study has revealed that there is an exceptional case (see Ref. 11). Some of the wave functions were proved to be localized in a power law with a self-similar structure and the exponents of the localizations were calculated; strictly speaking, they have a multifractal structure.[12] All the other states are chaotic or random. An interest-

ing fact is that the singular continuous spectrum and the power-law behaviors of the wave functions do not vanish no matter how small the quasiperiodic potential is, but the potential strength affects only the value of exponents. This is different from incommensurate systems such as the Harper model,[13] which changes its electronic properties with increasing incommensurate potential strength from extended wave functions and finite bandwidth to localized wave functions and zero bandwidth. This difference arises from the magnitudes of short-wavelength Fourier components of the quasiperiodic potentials. Since the short-wavelength components of the FC have larger amplitudes than those of the incommensurate models, the wave functions of the FC are more extended in the momentum space, and thus correspondingly localized in the coordination space.

We cannot, however, immediately regard all these electronic properties of the FC as universal in other QC, because this model is quite special in the QC family owing to its one dimensionality. The speciality of 1D systems is well known in the Anderson localization problem: the wave functions are always localized no matter how small the disorder strength is. But a more important point is that the FC lose the *topological* nonperiodicity, a characteristic feature of real QC materials in 3D. Actually, the quasiperiodicity of the FC model is not a topological one but the distribution of double-valued potentials (or transfer energies) on a topologically regular lattice. The topological nonperiodicity has a remarkable effect on the electronic properties—*frustration* of the wave functions,[14] which we will discuss later. Consequently, some of the results in the FC would be specific to 1D systems and the FC may not exhibit the electronic properties general in higher-dimensional QC. In order to study the electronic properties of QC from the viewpoint of the effect of topological quasiperiodicity, we must hence treat the systems in two or higher dimensions. We would like to clarify whether the properties observed in the FC are also generic in higher-dimensional QC by studying the Penrose lattices[15,16] (PL) as a typical 2D example.

In comparison with the FC, the PL has been studied by fewer researchers,[17] and mathematically rigorous results are only some exact eigenstates located at particular energies. First, it is known that the nearest-neighbor tight-binding models have thermodynamically degenerate eigenstates, called confined states and string states.[18–20] These states are strongly localized and their thermodynamic degeneracy is due to Conway's theorem. But they are not a characteristic property of QC in themselves, since they are a consequence of special local topology. In addition, their high degeneracy means that they are unstable to perturbations such as long-range electron transfers or nonuniform potentials;[21] note that the existence of the confined states strongly depends on the Hamiltonian. Therefore it may be an oversimplification to conclude that other wave functions have the same character. The second rigorous result is that we can construct a tight-binding Hamiltonian so that certain multifractal wave functions should be its eigenstates by setting long-range transfer energies according to a complex rule.[22] It is intriguing that this procedure can be applied to an infinite number of (but, of course, particular) multifractal wave functions. But since this procedure is quite artificial, it is not clear whether there are also multifractal eigenfunctions in other simple models, such as nearest-neighbor hopping models.

We will study the electronic properties of the PL in 2D in this paper and the following one (hereafter referred to as I and II). Paper I is devoted to the study of the electronic structure, mainly smoothness of the energy spectrum and localization problem of the wave functions. The subject of Paper II is the transport properties, particularly conductance at zero temperature, and discussion will be given based on the electronic structure studied in I. We hope to more deeply understand the effect of quasiperiodic lattice structure on the electronic properties. The PL are an appropriate model for that purpose due to their two dimensionality (the lowest-dimensional model with topological quasiperiodicity). One advantage is that lower-dimensional systems exhibit the effect of "disorders" on the electronic properties more clearly. Therefore the PL would be the model most sensitive to topological quasiperiodicity, one of whose important effects is frustration induced in phases of the wave functions. The other advantage is a practical one, tractability in numerical computations. A smaller number of sites are sufficient to reproduce the localization behavior in the PL compared to higher-dimensional models, since localization of wave functions would be determined by linear size of the systems.

This paper is organized as follows. In Sec. II we sketch our argument on general trends of the electronic properties of QC based on their quasiperiodic lattice structures. In Sec. III we explain the model Hamiltonian to be studied, with emphasis on the choice of boundary condition. In Secs. IV and V, we show results of numerical computations on the density of states (DOS) and the wave functions, respectively, and discuss the electronic properties. The last section is devoted to brief conclusions. In the Appendix, we review our method of generating periodic approximations of the PL in the framework of the multigrid method; these approximations are used as a structural template of the model Hamiltonian. Some results have been already published in letter form.[23,24] In this paper we would like to show our results and discussions more completely.

II. GENERAL ASPECTS OF ELECTRONIC STRUCTURE OF QUASICRYSTALS

In this section, we will consider general trends of the electronic structure of QC before numerical computations, focusing particularly on smoothness of the energy spectrum and localization behavior of the wave functions.

Let us first define our terminology about the energy spectrum and localization behavior to make our discussions clear. In discussing the singularity of the energy spectrum, we will sometimes use the term *smooth spectrum* to specify the spectrum in which all level spacings are scaled by the reciprocal of the site number, $\Delta E \propto 1/N$. On the other hand, we will call the spectrum with an anomalous system-size dependence, $\Delta E \propto 1/N^{\beta}$

($\beta \neq 1$), an *unsmooth spectrum* or *singular spectrum*. In describing localization behavior, let us define the wave functions which cannot be normalized in infinite systems but are not extended, as *critical wave functions*. Here, *extended wave functions* means that they have asymptotically homogeneous amplitudes, $\int_{|\mathbf{r}|<R} |\psi(\mathbf{r})|^2 d\mathbf{r} \sim R^d$ (d: space dimensions), while our definition of *localized wave functions* is square-integrable wave functions. Note that according to this definition, power-law wave functions $\psi(\mathbf{r}) \sim |\mathbf{r}|^{-\alpha}$ are classified into the localized wave functions if their exponent $\alpha > d/2$.

To argue the electronic structure, we should take into account two important properties which characterize QC structure; one is nonperiodicity and the other is the property known as Conway's theorem,[16] in the case of PL. Conway's theorem states any finite-size section of the lattice repeats its figure an infinite number of times quasiperiodically. (Hereafter we will also call this property by the name of Conway's theorem for other QC, for simplicity.) In the PL, its quasiperiodic structure is characterized by the golden ratio τ. Its irrationality leads to the nonperiodicity of the lattices and the quadratic identity $\tau^2 = \tau + 1$ creates the self-similarity and Conway's theorem. As we will discuss below, the nonperiodicity of QC has a tendency to cause the wave functions to be localized, while Conway's theorem leads them to be extended.[23]

It is appropriate to apply the picture of nearly free electrons—the approach from the limit of extended wave functions, in order to explain our argument that nonperiodicity of QC leads the wave functions to become localized. Now, assume the potential energy is proportional to the structure factor in the momentum space $V_{\mathbf{k}} \propto S(\mathbf{k})$, which assumption may be qualitatively valid. Remember that each spot $\mathbf{k}$ of the diffraction pattern opens an energy gap at the Bragg plane which bisects the line joining the origin to the point $\mathbf{k}$, and the energy dispersion jumps by an amount of about $2|V_{\mathbf{k}}|$ at the plane. On the other hand, once we recall the characteristic property of QC that the momentum space is densely filled with diffraction spots, we notice that the momentum space is densely filled by the Bragg planes and that the energy bands become shredded into tiny pieces with gaps opening at almost every $\mathbf{k}$ point. Considering that these gaps are associated with almost equal-weighted hybridization of the wave functions on the Bragg planes corresponding to $\mathbf{k}$ and $-\mathbf{k}$, the dense distribution of the Bragg spots implies that an unperturbed Bloch wave function will be hybridized with a number of wave functions with various momentums owing to the potential scattering. The hydridization in the momentum space leads to wave functions correspondingly localized in the coordinate space. Since the DOS is obtained by projecting the shredded energy dispersion curve into the energy space, it must have a singular part and cannot be very smooth. It should be emphasized that the singularity depends on lattice dimensionality, because energy degeneracy plays an important role in this mechanism in the sense that both energy and momentum must be conserved in the scattering process of a Bloch electron pair and the energy degeneracy depends on the space dimensions. In the case of the FC, as shown by Kohmoto *et al.* and Ostlund *et al.*,[8] the DOS has a self-similar hierarchy of energy gaps and the total bandwidth is zero in the thermodynamic limit, no matter how weak the quasiperiodic potentials are. In this case, gaps in the energy-momentum dispersion curve directly result in energy gaps in the DOS, and this comes from the one-to-one correspondence between energies and momenta, except the double degeneracy of $\mathbf{k}$ and $-\mathbf{k}$. On the other hand, in more than one dimension, an infinite number of unperturbed Bloch states with the same $|\mathbf{k}|$ are degenerate at a specified energy. While the energy is isotropic with respect to the direction of the momentum vector, the scattering potential $|V_{\mathbf{k}}|$ is anisotropic, actually decagonal in the PL. Therefore the gap does not open at all the points on the constant-energy surface and there still remains a part of the zero-gap surface. Of course, in the PL the gap structure also shows tenfold symmetry in the momentum space. The remaining zero-gap surface contributes to keeping the DOS finite at the specified energy, even though the value is considerably reduced. Actually, tenfold symmetry is close to being isotropic, but real gaps would not appear in the DOS in this sense, and only pseudogaps open. Thus, based on the intuitive argument above, we expect that QC have an unsmooth energy spectrum and localized wave functions, but the total bandwidth will be generally nonzero in more than one dimension, in contrast to FC.

Then are wave functions in QC exponentially localized? To discuss this question, we must take into account the effect of Conway's theorem that leads the wave functions to become extended. To illustrate this process, let us make a thought experiment based on the real-space renormalization-group (RSRG) theory starting from the opposite limit of the previous argument, i.e., the limit of localized wave functions. From now on we consider the case of the PL in particular, but the argument would hold in various kinds of QC. Suppose that there is an eigenstate whose eigenfunction can be well approximated by a wave function ψ_0 mostly localized in a section with radius ξ_0, i.e., its localization length is ξ_0. According to Conway's theorem, the section where ψ_0 is localized has some duplicates within a distance of $4\xi_0$.[16] Hereafter, we shall set the number of duplicates as 1 for simplicity, but this simplification does not lose generality. Put the same wave function as ψ_0 on the duplicate section by translation and call it ψ_0', then ψ_0' would be another good approximation of the specified eigenfunction as well as ψ_0. The energy difference between ψ_0' and ψ_0 is very small because it comes only from the difference of atomic configuration outside the finite sections,[25] and the overlap integral of the two wave functions ψ_0 and ψ_0' is in the order of $e^{-a\xi_0}$ where a is a constant close to 4. Thus the Hamiltonian with degrees of freedom limited to the two wave functions ψ_0 and ψ_0' can be described by a two-level system: the diagonal matrix elements are determined by the level separation between the two states, and the off-diagonal elements $\langle \psi_0 | H | \psi_0' \rangle$ are in the same order as the overlap integral. By diagonalizing the Hamiltonian, we can obtain two better approximations of the specific

eigenfunction—bonding and antibonding states made of ψ_0 and ψ_0', and their localization lengths become longer in the order of the distance between the two patterns $\xi_1 \sim a\xi_0$. Because Conway's theorem holds for any pattern, we can repeat the above RSRG procedure an infinite number of times. This means that the localization length will diverge with the number of RSRG procedures. Consequently, wave functions cannot be localized exponentially in QC in general, but would show power-law decays instead. If the amplitude of the wave functions and the length scale vary with the RSRG step as $\psi \sim c^n$ and $L \sim a^n$, the exponent of power-law decay is given by $-\ln c/\ln a$. In fact, in the FC some of the wave functions show power-law decays (strictly speaking they have multifractal structure[10] and others are also believed to be critical). The difference between QC and other materials lies in the magnitude of the matrix elements. Of course, periodic crystals have self-similarity as well as QC and Conway's theorem holds in them. But because their lattice structure is really periodic, the two diagonal elements of the effective two-level Hamiltonian always have the same value and this results in $c=1$. Consequently, the exponent becomes zero, as required by Bloch's theory. On the other hand, since disordered materials have no restrictions on distribution of potential energies in the lattice, duplicates of a finite pattern locate very far from the original one; roughly speaking, the distance increases exponentially with respect to the diameter of the pattern, while it is proportional to the diameter in QC. As a result, the off-diagonal elements of the effective two-level Hamiltonian of disordered systems are much smaller than the level separation, and hence the two states cannot hybridize well. This means the wave functions must be localized exponentially.

In conclusion, power-law decays are caused by competition of the two effects of QC—nonperiodicity and self-similarity (Conway's theorem), which have a tendency to lead the wave functions to be localized and extended, respectively. Of course, our argument is not mathematically rigorous but only heuristic and qualitative. To verify our scenario analytically, a perturbation theory for a dense set of potentials $\{V_{\mathbf{k}}\}$ ranging over many orders in magnitude is necessary, but no one has yet succeeded in that difficult problem in more than one dimensions.[26,27] Therefore, by direct numerical computation we will study the energy spectrum and the wave functions of the PL to confirm our scenario.

III. MODEL

We will explain the model studied, and comment on some of its properties which are obtainable without numerical computations. Appropriate models should be Hamiltonians simple but sufficient to reproduce the characteristic properties of QC, and it is desirable that the number of free parameters be small. An important consideration is the choice of boundary condition to use in numerical computations.

Our model is a single-band tight-binding Hamiltonian on the PL in which an s-like atomic orbital is placed in the *center* of each rhombus and the transfer energies are set to be finite and constant only between nearest-neighbor rhombus pairs irrespective of their distances. We choose the transfer energy as -1 so that slowly varying wave functions should have lower energies, then the eigenvalue equation is

$$(H\psi)_i = -\sum_{\langle i,j \rangle} \psi_j = E\psi_i \ , \tag{3.1}$$

where the sum is taken over the nearest-neighbor sites of the site i. Although our model is not realistic for studying physical properties of real QC materials such as Al-Mn alloys (e.g., the conduction band is not an s band but is made up of Al's $3p$ and Mn's $3d$ orbitals), we believe it adequate to qualitatively consider the effect of quasiperiodicity on the electronic structure. Our model has no free parameter, i.e., all the energies are scaled by the transfer energy, and quasiperiodicity is taken into account through the connectivity of the sites in the Hamiltonian. Considering this point, we may hence expect that there would be no critical energy at which the spectrum changes its character and that the character would be qualitatively the same everywhere in the spectrum. We will discuss this point again when we analyze the DOS through approximated band calculations.

Here, we list the structural properties of our model.

(i) The coordination number is 4 at all the sites.
(ii) The lattice is not bipartite.
(iii) There is a majority of odd-member rings in the ring statistics (87.5%).

From these properties, we can easily obtain information on the electronic structure.

(1) The eigenvalues are restricted within the region $-4 \le E \le 4$.

(2) The DOS is asymmetric.

(3) At the band bottom $E=-4$, our model has the eigenstate with uniform amplitudes, i.e., the totally bonding state, like the square lattice.

(4) Antibonding states near the band top are strongly frustrated owing to the odd-member rings, so the band top is pushed down some degree from $E=4$.

Another model has been used in some studies,[17,19,20] a tight-binding Hamiltonian where an atom is placed on each *vertex* of the rhombuses instead of on the center. In that model, the lattice is bipartite but the coordination number ranges from 3 to 7; as a result, the DOS is symmetric and the eigenenergies are distributed within the region $-7 \le E \le 7$. Since the coordination number varies from site to site, the wave functions of the eigenstates near the band edges have large amplitudes on the sites with large coordination numbers. On the other hand, in our model this mechanism does not work, because the coordination number is constant.

We must overcome two difficulties to perform numerical computations. First, since we can manipulate only finite systems, not infinite systems, a systematic extrapolation of the results obtained for several finite systems is indispensable for understanding thermodynamic behaviors. However, because QC do not have unit cells, a finite part of a QC of a fixed size does not have a uniquely

determined atomic configuration. In this sense, it is difficult to perform "systematic" calculations in QC, in contrast to crystals. What is the most systematic procedure to reach an intrinsic QC?

The second point is that the boundary condition is an important consideration when we study the electronic structure or the transport properties. It is well known that a surface of a lattice creates surface states localized near the surface (their number is proportional to the surface area), and they are sensitive to the boundary condition in use. In the thermodynamic limit, the surface states do not contribute to bulk properties, i.e., extensive quantities such as specific heat, susceptibility, etc., but they affect transport properties more seriously. A more important point is that the systems which we can treat in numerical computations are not extremely large (roughly speaking, fewer than 10^3-10^6 sites), hence we should make every effort to reduce the boundary effects. What is the best boundary condition to this end? Presumably the best choice would be the periodic boundary condition. If the Dirichlet boundary condition were imposed, a number of atoms would be exposed to the vacuum and electrons on these atoms could not move towards that direction. On the other hand, if we can impose the periodic boundary conditions (as we explain below, this is possible with some modification), the local atomic environment of any atom in the finite lattice will be the same as in infinite lattices up to the distance of half of the linear lattice size.

The periodic boundary condition cannot be imposed originally, since QC do not have periodicity. However, we can show that it is possible to generate a sequence of periodic lattices that approximate a QC in a systematic way,[28,29] since QC have some structural properties similar to crystals. This method essentially relates to the optimal rational approximants of the irrational number which characterizes the QC structure. The systematic sequence of the periodic approximated lattices is also an answer to the first problem of how to extrapolate to the thermodynamic limit. We generated periodic approximations of the PL by modifying the pentagrid method,[23] and we will call these *the periodic Penrose lattices* (PPL) hereafter. Typical examples are shown in the Appendix, and we review our generation method and analyze their structure there. We note that the PPL are very close to the original PL: actually, the number of defects in the unit cell, i.e., wrong edges where Penrose's matching rule is violated, can be reduced to 2, irrespective of unit-cell size.[29] Hence our Hamiltonian with the periodic boundary conditions reproduces the same local atomic configuration as the original PL except at the two defects as far as the unit cell is concerned, and it will converge to the thermodynamic limit faster than the models with the Dirichlet boundary conditions, where all the sites on the free surface are defects.

We diagonalize the tight-binding Hamiltonian defined for unit cells of the PPL by imposing the periodic boundary conditions in two directions of the translation vectors, but do not perform the band calculation by continuously varying the wave vector in the Brillouin zone. It is possible in principle to calculate energy dispersions $\{\varepsilon_k\}$ for the periodic lattice tiled by the unit cell, but we think it would be neither useful nor practical. If we improve the periodic approximation of the lattice by one step, the area of the Brillouin zone will be reduced by a factor close to τ^{-2}, and the energy bands will become folded and divided into subbands. Thus the point $\mathbf{k}=\mathbf{0}$ of a large system corresponds to finite $\mathbf{k}$ points of a smaller system. Therefore we had better calculate for large systems with the periodic boundary condition rather than calculate for small systems at finite $\mathbf{k}$ points. The main reason is the limit of computer time, however, so we calculate an approximated DOS using four boundary conditions instead.

IV. ENERGY SPECTRUM

We show in Fig. 1 the integrated DOS of the PL. They are straightforwardly obtained from the eigenenergies $\{\varepsilon_j\}$ calculated by numerical diagonalization of the Hamiltonian. The systems used here are 5 unit cells of the PPL generated with approximants $\tau\to\frac{3}{2},\frac{5}{3},\frac{8}{5},\frac{13}{8},\frac{21}{13}$; the lattice widths are $M=10,16,26,42,68$, and the site numbers are $N=76,199,521,1364,3571$, respectively. The reason we do not show the DOS itself is that it looks smooth or spiky depending on the width of broadening artificially introduced to draw the DOS curve. As seen in Fig. 1, the integrated DOS converges rapidly with increasing system size and we notice some features of the curves. (1) The DOS is not a Cantor set with hierarchical gap structure, and neither does it have large energy gaps. Some small gaps seem to exist, and we will discuss this point again later. (2) The band bottom remains at $E=-4.0$, and the corresponding wave function has uniform amplitudes in the coordinate space; on the contrary, the band top is pushed down to $E=2.68$. Remember,

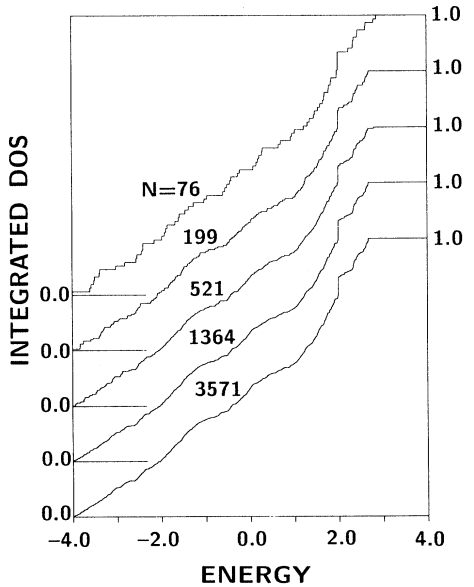

FIG. 1. Integrated DOS of the unit cells of five PPL under the periodic boundary conditions.

the coordination number is 4 at every site in our model, so that the feature at the band bottom is a natural consequence. The pushdown of the band top is caused by frustration of the antibonding wave functions at the odd-member rings in the atomic configuration, as explained in Sec. III. (3) The integrated DOS jumps exactly at $E=2.0$ by about 6.8%. This means that a thermodynamic number of the eigenstates are degenerate at this energy. They are the confined states and string states mentioned before. The analytical form was completely obtained for all of them:[18] they are unusual wave functions that have their amplitudes only on finite sections (the confined states) or on sections with the Hausdorff dimension $\ln 2/\ln\tau$ (the string states). Though their singular forms are interesting, they are not typical wave functions of QC, because the quasiperiodicity is not essential for their existence and they appear only at $E=2$ as discussed before. Therefore we will not investigate them further.

Next, we will study the smoothness of the energy spectrum by level statistics.[30] We actually calculate two quantities to measure the smoothness. First, consider the distribution of the level spacings ΔE between neighboring eigenstates and count the number of $\Delta E \le BN^{\beta}$:

$$D(\beta)\equiv\frac{1}{N-1}\sum_{j=1}^{N-1}\theta\left[\beta-\log_N\left[\frac{\varepsilon_{j+1}-\varepsilon_j}{B}\right]\right], \tag{4.1}$$

where N is the number of sites, $B\equiv\varepsilon_N-\varepsilon_1$ is the total band, and $\theta(x)=1$ if $x>0$ and 0 otherwise. The proportion of the level spacings with the system size dependence $N^{\beta}\sim N^{\beta+\Delta\beta}$ is given by $D(\beta+\Delta\beta)-D(\beta)$, so $D(\beta)$ is the integrated distribution function of the exponents β which specify the system-size dependence of the level spacings. Second, let us define another quantity with which to measure the smoothness of the DOS. Calculate the percentage of the energy regions filled by the level spacings with the size $\Delta E=BN^{\beta}$:

$$F(\beta)\equiv\frac{1}{N-1}\sum_{j=1}^{N-1}(\varepsilon_{j+1}-\varepsilon_j)\times\theta\left[\beta-\log_N\left[\frac{\varepsilon_{j+1}-\varepsilon_j}{B}\right]\right]. \tag{4.2}$$

This means that the fraction $F(\beta)$ of the total band B is filled by the level spacings with the size BN^{α} ($\alpha\le\beta$). In the thermodynamic limit, these functions should satisfy the following relations because B is independent of the system size: $D(\beta)=1$ when $\beta>-1$, and $F(\beta)=0$ when $\beta<-1$. It should be emphasized that these relations must be satisfied whether the DOS is smooth or singular. Before calculating them for the PL, let us consider the general behaviors of $D(\beta)$ and $F(\beta)$ curves in conventional systems. In the systems where the DOS, $\rho(E)$, is well defined and smooth, such as periodic crystals, the number of states locating within a small energy section from E to $E+\delta E$ is $N\rho(E)\delta E$, where N is the total number of sites. Then, the mean level spacing is given by $\overline{\Delta E}\sim\delta E/[N\rho(E)\delta E]=1/[N\rho(E)]$, so the system dependence is $1/N$, and consequently the exponent takes the value $\beta=-1$ for almost all states. On the other hand, in disordered systems where the eigenenergies are randomly distributed with no correlations, it is known that the level spacings follow the Poisson distribution with the width proportional to $1/N$.[31] Almost all level spacings are consequently scaled by $1/N$ and the result again is $\beta=-1$. Thus both in periodic crystals and in disordered materials, the two curves $D(\beta)$ and $F(\beta)/B$ must jump from 0 to 1 at $\beta=-1$ with increasing β, in the thermodynamic limit $N\to\infty$. Even if there is thermodynamic degeneracy at some energies, it will not change their character qualitatively: the only change to occur is the shrinkage of the jump at $\beta=-1$. The finite-size effect results in smooth increases in the curves instead of abrupt jumps, and the width of broadening decreases in proportion to $1/\ln N$ with increasing system size.

In Fig. 2, we show the $D(\beta)$ and $F(\beta)$ curves for the five PPL calculated by the data shown in Fig. 1. Curves with the smaller steps show the results of the larger systems. First, focus on the $D(\beta)$ curves. We observe that they have almost converged when $\beta<-1.1$ within these system sizes, and we may hence expect the $D(\beta)$ curve will smoothly decrease with decreasing β in this region in the thermodynamic limit. The smooth decrease of the curve in the region $\beta<-1$ means that a thermodynamic number of the level spacings have an anomalous size

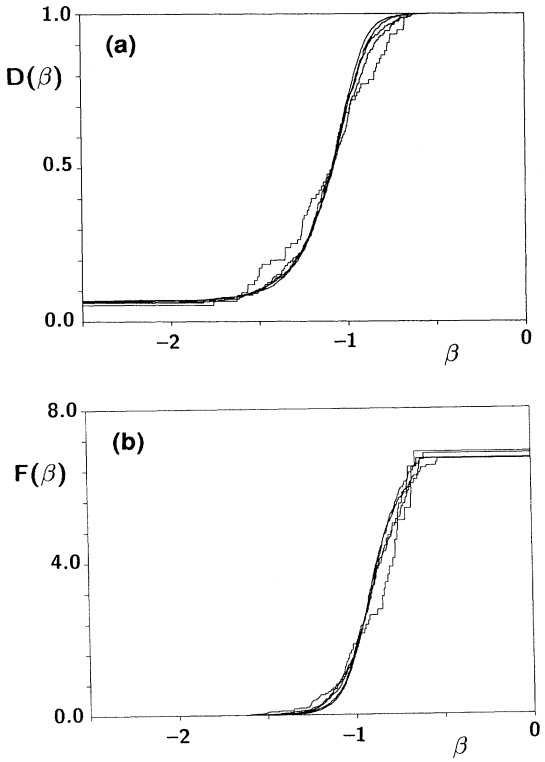

FIG. 2. (a) Integrated distribution of the system size dependence exponents of the level spacings, $D(\beta)$, and (b) integrated width $F(\beta)$. The systems are the PPL unit cells with $N=76,199,521,1364,3571$, and curves with smaller steps are for the larger systems. The total band B is fixed to the estimated limit value $B_{\infty}=6.68$.

dependence—a width narrower than conventional systems. In other words, the DOS has a singular part: it will diverge at those energies. On the other hand, the curve approaches $D(\beta)=1$ in the region $\beta>-1$ with increasing system size, as required by the general relation. We comment on the finite value of the $D(\beta)$ curve at very low β. It comes from the thermodynamic degeneracy of the confined states and the string states, and actually the value agrees with the analytical estimation 6.68%.[18]

Next, let us focus on the $F(\beta)$ curves. Judging from the graph, we can expect that these curves show different behavior from conventional systems as well as the $D(\beta)$ curves and they converge into a continuously increasing curve when $\beta>-1$, although the convergence is not good within the present calculations. If the $F(\beta)$ curve shows the singular behavior as predicted here in the thermodynamic limit, a finite fraction of the band is filled by the level spacings with the size dependence wider than $1/N$. This means again that the DOS has a singular part: it will vanish at an infinite number of energy points. Note that the proportion of the anomalously large level spacings is, of course, zero.

Thus those anomalous $D(\beta)$ and $F(\beta)$ curves illustrate the unsmooth character of the DOS. Actually, it is expected in the limit of $N\rightarrow\infty$ that a thermodynamic number of level spacings have the system-size dependence narrower than the smooth spectrum cases ($\beta<-1$) and that a finite part of the total band is filled with the level spacings with a size dependence wider than the smooth spectrum cases ($\beta>-1$). These behaviors indicate that the energy spectrum of the PL is not smooth, in the sense of the definition in Sec. II. The exponent of system-size dependence β is continuously distributed.

Whether the DOS has a regular part or not is determined by the jump of the two curves at $\beta=-1$. If the $D(\beta)$ and $F(\beta)$ curves jump by finite amounts there, the DOS has a regular continuous part in addition to a singular part. We cannot judge whether there is a regular part within the present calculation, but the conclusion can remain that the DOS has a singular part.

We will try an approximated band calculation to visualize the singular part of the DOS more clearly. As explained before, the band calculation is possible in principle due to the lattice periodicity, but almost untractable for large systems because of the limitation of computer time. We calculate the DOS using the eigenenergies only at four $\mathbf{k}$ points, but this analysis is sufficient to reproduce its unsmooth character qualitatively. Our method is as follows. Choose the four $\mathbf{k}$ points at $\mathbf{0}$, $\mathbf{b}_1/2$, $\mathbf{b}_2/2$, and $(\mathbf{b}_1+\mathbf{b}_2)/2$ where $\mathbf{b}_1$ and $\mathbf{b}_2$ are the reciprocal lattice vectors of each PPL, and approximate each band by constant DOS. One reason for this choice is that extreme points in the energy dispersion curves usually appear at high symmetry points in the Brillouin zone. Term the eigenenergies at the four $\mathbf{k}$ points $\{\varepsilon_{i\Gamma}\}$, $\{\varepsilon_{iX}\}$, $\{\varepsilon_{iY}\}$, and $\{\varepsilon_{iM}\}$, respectively, then the approximated DOS is given by

$$\rho(E)=\frac{1}{N}\sum_{i=1}^{N}\frac{1}{\varepsilon_i^{\max}-\varepsilon_i^{\min}}\theta(E-\varepsilon_i^{\min})\theta(\varepsilon_i^{\max}-E)\ , \qquad (4.3)$$

where $\varepsilon_i^{\min}\equiv\min\{\varepsilon_{i\Gamma},\varepsilon_{iX},\varepsilon_{iY},\varepsilon_{iM}\}$, and $\varepsilon_i^{\max}\equiv\max\{\varepsilon_{i\Gamma},\varepsilon_{iX},\varepsilon_{iY},\varepsilon_{iM}\}$. Here, we assume that there are no level crossings, and this assumption is generally valid except for accidental degeneracies because our unit cells have almost no symmetries. (In fact, the unit cells used here have mirror symmetry with respect to the diagonal line, but it leads only to the degeneracy of $\varepsilon_{iX}=\varepsilon_{iY}$ and does not refute the above argument.)

We show the results of the DOS in Fig. 3 and they reveal two characteristic features. One is that the DOS becomes less smooth and more spiky with increasing system size. This feature confirms our conclusion that the DOS has a singular part, since it would otherwise converge into a smooth curve. The other is that the smoothness depends on energy regions. At low energies, each band is quite broad and several bands overlap each other; accordingly the DOS is relatively smooth. On the other hand, at high energies the bands hardly overlap and the width of each band is narrow, consequently the DOS looks spiky. The energy dependence of the smoothness is consistent with behaviors of the wave functions calculated by numerical diagonalization. At low energies, the wave-function amplitudes vary slowly in the coordinate space and are similar to plane waves. As a result, their energies vary by considerable amounts depending on the boundary conditions. At high energies, the phase of the wave functions oscillates rapidly in the coordinate space and the phase correlation length is quite short; consequently, the eigenenergies are not much influenced by the boundary conditions. These behaviors explain the difference of the DOS character between low- and high-energy regions. When we explained our model in Sec. II, we expected that the character of the energy spectrum would not change in the band because our model has no free parameters. Hence, if the spectrum intrinsically changes in smoothness or has any energy gaps, they must originate from the scattering by topological nonperiodicity and the coherent interference effect of multiple-scattered waves would cause this. But the smooth DOS in the low-energy region might be a finite-size effect, since the slowly varying wave functions in this energy region suggest that the lattice used here might not be large enough. We cannot judge whether the energy spectrum retains a smooth character in the thermodynamic limit or whether it also becomes singularly unsmooth. In any event, it is true that the degree of smoothness is relatively different between the low- and high-energy regions. We will discuss this problem again in Paper II, based on the dependence of conductance on energy and lattice length. We note that actually there is a 2D quasiperiodic model which intrinsically changes the character of its electronic structure from extended to critical.[32] But this model has a parameter which measures the strength of the quasiperiodic potential, and the character changes with respect to this parameter. Therefore this example does not necessarily support the change of the DOS character in the PL model.

The approximated DOS supplies another important piece of information on the total bandwidth. Our conclusion that the DOS of the PL is not a Cantor set and has a finite bandwidth was based on the integrated DOS

curve profile, but we can discuss this point more quantitatively by analyzing the approximated DOS shown in Fig. 3. We directly calculate the total bandwidth by summing up the area of the energy regions within the spectrum. The result for the system with $N=3571$ is (the total bandwidth)$/B=0.62$, where again $B=\varepsilon_N-\varepsilon_1$, and its system-size dependence is small in contrast to the FC model. This result explicitly shows that the energy spectrum of the PL occupies a finite energy region—an important difference between 1D and higher-dimensional QC.

A comment on our band calculation to avoid possible misunderstanding: we calculated eigenenergies at four points in the Brillouin zone of the PPL, but of course the Brillouin zone cannot be defined for the original PL because it has no periodicity. The approximated band calculation is an analysis to study the thermodynamic limit behaviors of the DOS from the results of finite systems, and we believe the results of this analysis are reliable and useful even when the systems in use are not very large.

V. WAVE FUNCTIONS

We will study the localization problem in the PL in this section. We argued that the wave functions should be critical in the sense defined in Sec. II, based on a heuristic argument. We investigate this problem by calculating the $2p$ norm of the wave functions defined as follows:

$$\|\psi\|_{2p}\equiv\frac{\sum_n|\psi_n|^{2p}}{\left(\sum_n|\psi_n|^2\right)^p}\ . \tag{5.1}$$

This is a generalization of the participation ratio,[33,34] which corresponds to the particular case of $p=2$. It satisfies the axioms of norm only if $p\geq 1$, but we may use it as the measure of localization irrespective of p. To apply this quantity to the localization problem, calculate the $2p$ norm in a section of N sites for power-law functions $\psi(\mathbf{r})\sim|\mathbf{r}|^{-\alpha}$ in 2D, then the result is, when $p>1$,

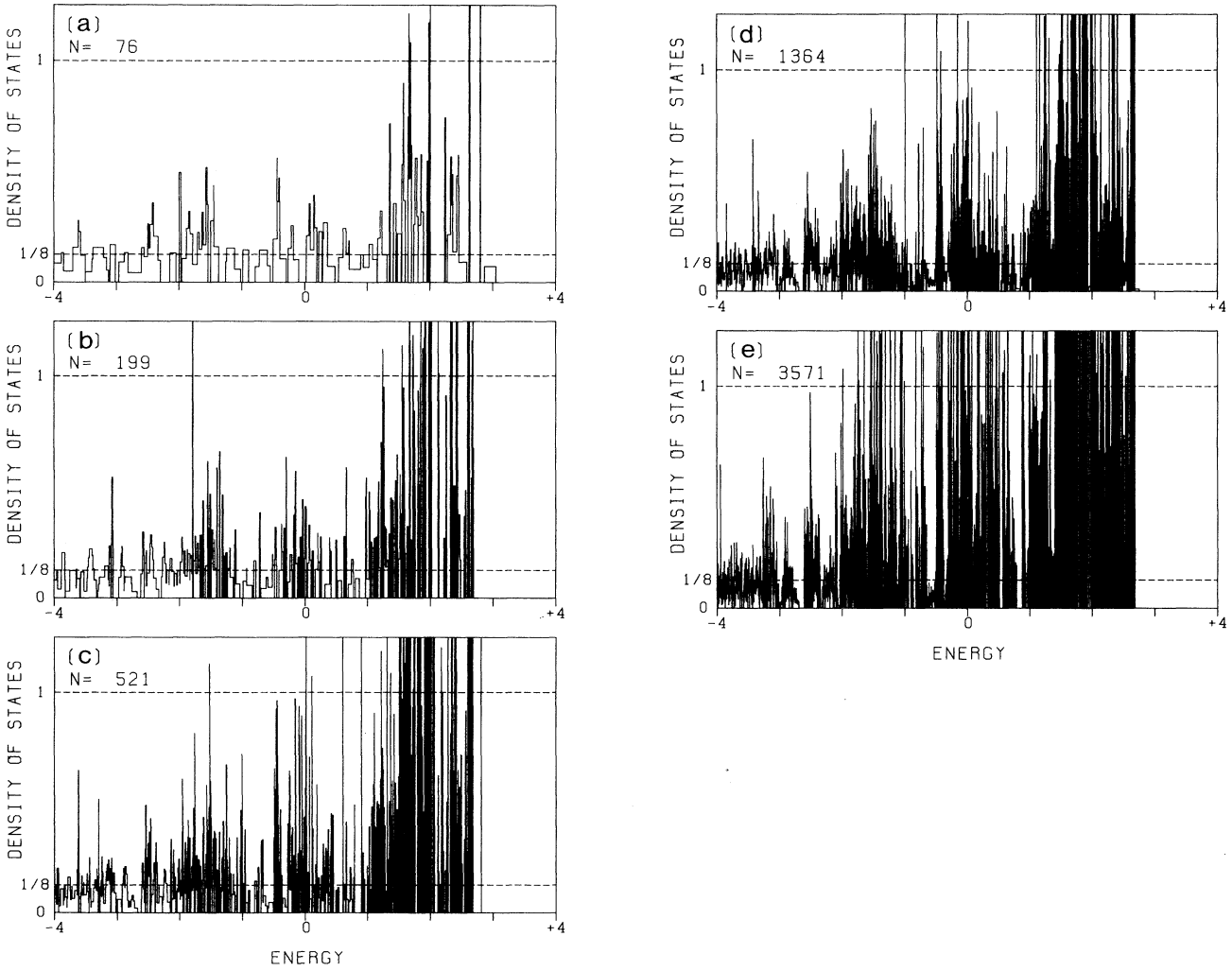

FIG. 3. Approximated DOS of the PPL calculated from the eigenenergies at four **k** points.

$$\|\psi\|_{2p} \simeq \begin{cases} N^{-(p-1)} & (0 \le \alpha < 1/p) \\ N^{-p(1-\alpha)} & (1/p \le \alpha < 1) \\ N^0 & (1 \le \alpha) , \end{cases} \tag{5.2a}$$

and when $p < 1$,

$$\|\psi\|_{2p} \simeq \begin{cases} N^{1-p} & (0 \le \alpha < 1) \\ N^{1-\alpha p} & (1 \le \alpha < 1/p) \\ N^0 & (1/p \le \alpha) . \end{cases} \tag{5.2b}$$

Therefore we can obtain the exponents of the wave functions by analyzing the system size dependence of the $2p$ norms calculated in systems of sufficient size. For exponents $\alpha < 1$ ($\alpha > 1$), the parameters of $p > 1$ ($p < 1$) are appropriate choices for the $2p$-norm analysis. Exponentially localized wave functions give the value $\|\psi\|_{2p} \simeq N^0$ and freely extended wave functions correspond to the case of $\alpha = 0$.

We show in Fig. 4 the integrated distribution function of the 8 norm calculated for all the wave functions of the four PPL with the site numbers $N = 76, 199, 521, 1364$. The PPL with $N = 3571$ is not calculated owing to limited computer time. The integrated distribution function is defined by

$$I(\gamma) \equiv \frac{1}{N} \sum_{n=1}^{N} \theta(\gamma - \log_N \|\psi^{(n)}\|_8) . \tag{5.3}$$

The $I(\gamma)$ curve shows the integrated distribution of the exponents of power-law decays for a specified system if the finite-size correction is negligible. Since we set $p = 4$, the value γ is related to the localization exponent α as $\alpha = 1 + \gamma/4$ when $-3 < \gamma < 0$ [see Eq. (5.2a)]. An advantage of the $2p$ norm is that the analysis can be applied for any power-law wave functions by setting p at a suitable value according to the power-law exponent α. The global profile of the $I(\gamma)$ curve has not converged sufficiently, but since the discrepancy between the largest two systems is quite small, particularly at low γ, we can expect the result of the system with $N = 1364$ to be close to that in the thermodynamic limit, and that the $I(\gamma)$ curve will show a smooth increase with γ mostly in the region $-\frac{5}{2} < \gamma < -\frac{3}{2}$. This behavior means that most of the eigenfunctions in the PL are power-law localized in the space with the exponents $\frac{3}{8} < \alpha < \frac{5}{8}$. Since the power-law decaying functions with the exponent $\alpha < 1$ cannot be normalized as mentioned in Sec. III, they are classified as critical wave functions. Since critical wave functions do not correspond to the point spectrum part of the DOS, the result of the 8 norm supports our conclusion on the singularity unsmooth energy spectrum.

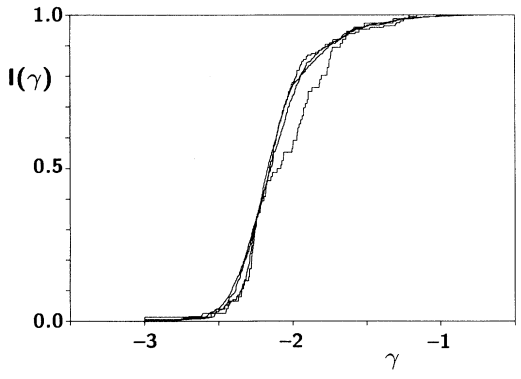

FIG. 4. Integrated distribution of 8 norms of the eigenfunctions, for four PPL with $N = 76, 199, 521, 1364$. Curves with smaller steps are for the larger PPL.

Thus we have succeeded in confirming the critical character of the wave functions and the localization exponents are determined as $\frac{3}{8} < \alpha < \frac{5}{8}$ through an analysis of the 8 norm. However, the absolute values are not so reliable, because the lattices used here are sometimes not large enough to reproduce asymptotic behaviors of the 8 norms. This effect brings finite-size correction to the exponents, and, in particular, we must take into account the fact that wave functions have nodes. But since the exponents are shifted to larger values by the effect of the nodes, we can expect the real values are smaller than those obtained here, and consequently the present conclusion on the critical wave functions is unchanged. We will discuss the absolute values of the exponents again in Paper II, based on length dependence of the conductance.

Note that we should take care in the interpretation of the power-law decays. The $2p$ norm defined above is determined only by the distribution of amplitudes of the wave functions, and the information on spatial form of the wave functions is not included in the formula of the $2p$ norm. Therefore, what we call power-law wave functions here are not necessarily the functions whose envelope functions decay in a power law. We cannot rule out anomalous cases such as wave functions whose amplitudes obey the same distribution function as the power-law function but are distributed randomly in the coordinate space, nor can we distinguish single power-law wave functions and self-similar wave functions with multifractal structures.

VI. CONCLUSIONS

In this paper we have studied the electronic structure of the Penrose lattice by the numerical diagonalization of a nearest-neighbor tight-binding Hamiltonian defined on a systematic sequence of approximated periodic lattices with up to 3571 sites. We investigated, in particular, smoothness of the energy spectrum and the localization problem of the wave functions by analyzing statistics of the level spacings and the $2p$ norms, respectively. We thereby found that the energy spectrum contains a singular part in spite of its finite total bandwidth, i.e., energy separations have anomalous system size dependence, and that most of the wave functions are critical and have a similar behavior to the power-law decaying functions with the exponents $\frac{3}{8} - \frac{5}{8}$. These numerical results support our heuristic arguments that the electronic structures of quasicrystals generally also exhibit singular behaviors in higher than one dimension due to the competition between the localization and delocalization mechanisms originating from two characteristic structural

properties. Further analysis and discussion will be made in Paper II by studying their transport properties.

ACKNOWLEDGMENTS

The authors thank Yukio Konishi for discussion on the $2p$ norms. This work was partly supported by a Grant-in-Aid for Scientific Research on Priority Areas, "Quasicrystals," from the Ministry of Education, Science and Culture of Japan.

APPENDIX: PERIODIC APPROXIMATIONS OF THE PENROSE LATTICE

In this appendix, we explain our method of generating periodic approximations of the PL in the framework of the multigrid method originally proposed by de Bruijn.[35] In some other works, similar approximations based on the projection method have been proposed, particularly for describing modulated 3D structure,[28,29] but as de Bruijn[35] and Gähler and Rhyner[36] showed, these two methods are equivalent. The emphasis is put on the unified prescription of the approximations modified in one direction and those in two directions.

1. Multigrid method

First, we review briefly the multigrid method[35] of generating the PL and define the technical terms which we will use later. In terms of the multigrid method, a PL tiled by two kinds of rhombuses (fat and thin) is topologically described as the dual lattice of a pentagrid. A *pentagrid* G is an ensemble of five sets of equally spaced parallel lines, and each set of parallel lines G_j is called a *grid*:

$$G=\bigcup_{j=1}^{5} G_j \ , \tag{A1a}$$

$$G_j=\{\mathbf{x}\in\mathbb{R}^2 | \mathbf{x}\cdot\mathbf{e}_j=k_j+\gamma_j,\ k_j\in\mathbb{Z}\} \ , \tag{A1b}$$

$$\mathbf{e}_j=(\cos(j-1)\phi,\ \sin(j-1)\phi),\quad \phi=2\pi/5 \ , \tag{A1c}$$

where $\mathbb{R}$ and $\mathbb{Z}$ are the sets of all real numbers and all integers. The five real parameters $\{\gamma_j\}$, called *grid parameters,* specify the position of the origin of the pentagrid, and must be chosen to satisfy the relation $\sum_j \gamma_j=0$ (mod 1) and so that any set of the three lines should not cross at a single point. The five unit vectors $\{\mathbf{e}_j\}$, pointing to the vertices of a regular pentagon, determine the direction and the spacing of each grid G_j, and are called *grid vectors.* The pentagrid divides the grid space into small pieces in the shape of polygons. The PL are generated by mapping these polygons into rhombus vertices in the physical space, and these two lattices are consequently dual to each other. The method of mapping is as follows. For each piece in the grid space, let us define a set of five integer indices:

$$K_j(\mathbf{x})=\lfloor \mathbf{x}\cdot\mathbf{e}_j-\gamma_j \rfloor \quad (j=1,\ldots,5) \ , \tag{A2}$$

where $\mathbf{x}$ is taken inside the piece and $\lfloor x \rfloor$ denotes the largest integer less than or equal to x. Next, assign the piece a 2D vector by

$$\mathbf{P}(\mathbf{x})=\sum_{j=1}^{5} K_j(\mathbf{x})\mathbf{t}_j \ , \tag{A3}$$

then, this vector gives the coordinate of the corresponding rhombus vertex. Here, $\{\mathbf{t}_j\}$ are called the *tiling vectors* and usually chosen to be $\mathbf{t}_j=\mathbf{e}_j$. Finally, determine the connectivity of the vertices as follows. Consider an intersection of the lines in the grid space, then notice that it is shared by just four polygons and they are mapped into four vertices in the physical space as stated above. Connect each vertex pair whose corresponding polygons share an edge, and a rhombus is obtained. Generating rhombuses for all intersections in the pentagrid, we obtain a PL tiled by thick and thin rhombuses without any overlap or vacancy. We note an important property of the PL which we will use in a numerical calculation scheme in Paper II. Each grid of the pentagrid is mapped into quasiperiodically spaced rhombus arrays in the physical space. In each array, rhombuses line up sharing two opposite sides with their two neighbors. Because each rhombus has two pairs of parallel sides, it lies on the corresponding two grids.

2. Periodic approximations

Periodic approximations of the Fibonacci chain have been used for systematic calculations of electronic properties.[8] However, we cannot impose the periodic boundary conditions on arbitrarily chosen parts of 2D or 3D quasiperiodic lattices. But since the PL consist of grids as well as crystals, we can generate their periodic approximations with certain modifications.

Our goal is *periodic pentagrids* which approximate the original one. Once they are given, periodic approximations of the PL can be straightforwardly constructed as their dual lattices. The nonperiodicity of the PL comes from the property that any two grids in the pentagrid form a rhombus lattice, but the other three grids are incommensurate to this lattice. Considering this point, our approximation method is (1) fix two grids as in the original pentagrid; (2) change the directions and the spacings of the other three grids so that they will be commensurate to the lattice made of the fixed two grids.

We can satisfy this requirement in the following way. Figure 5 shows the central part of the original pentagrid for grid parameters $\gamma_j=0$ for all j. (This choice is used only for judging whether they are commensurate or not. We will use appropriate parameters in actual lattice generation.) The five solid lines show the lines $\mathbf{x}\cdot\mathbf{e}_j=0$, and dashed lines $\mathbf{x}\cdot\mathbf{e}_j=1$. We shall fix the grids 1 and 2 hereafter, and they form a rhombus lattice tiled by a unit cell $OACB$ with the edge length $1/\sin\phi\equiv a$. Let P_j and Q_j be the intersections of the line $\mathbf{x}\cdot\mathbf{e}_j=1$ $(j=3,4,5)$ with OA and OB, respectively. In the case of the original pentagrid,

$$\overline{OP_3}=\overline{OP_4}=\overline{OQ_4}=\overline{OQ_5}=\tau a \ , \tag{A4a}$$

$$\overline{OP_5}=\overline{OQ_3}=a \ . \tag{A4b}$$

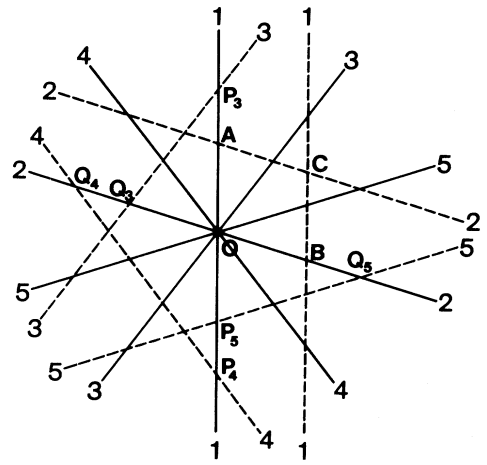

FIG. 5. Central part of the pentagrid when all $\gamma_j=0$.

Here, the irrational number τ in Eq. (A4a) is the reason that the grids $j=3,4,5$ are incommensurate with respect to the rhombus lattice made of grids 1 and 2. Therefore a periodic approximation of the pentagrid can be obtained by substituting rational numbers for the τ's, and this approximation is explicitly expressed by the grid vectors,

$$\tilde{\mathbf{e}}_1=\mathbf{e}_1,\quad \tilde{\mathbf{e}}_2=\mathbf{e}_2,\quad \tilde{\mathbf{e}}_3=-\mathbf{e}_1+\frac{1}{r_3}\mathbf{e}_2\ ,$$
$$\tilde{\mathbf{e}}_4=-\frac{1}{s_4}\mathbf{e}_1-\frac{1}{r_4}\mathbf{e}_2,\quad \tilde{\mathbf{e}}_5=\frac{1}{s_5}\mathbf{e}_1-\mathbf{e}_2\ , \tag{A5}$$

where the r's and s's are rational approximants of τ in the coefficients of OP's and OQ's, respectively. The grid spacing for $j=3,4,5$ is no longer 1 after the approximation.

Now that we have periodic pentagrids, we can generate periodic approximations of the PL by following the mapping procedure explained earlier. The grid parameters $\{\gamma_j\}$ must be chosen under the same constraints as before. Note that the tiling vectors are not modified but set to be $\mathbf{t}_j=\mathbf{e}_j$ as in the original PL case. This choice of $\{\mathbf{t}_j\}$ ensures that the generated lattices are tiled by the same thick and thin rhombuses as the original ones. Thus the independence of the tiling vectors from the grid vectors plays an important role in generating various modulated structures.

Some comments on the approximation are appropriate. The method (A5) does not cover all the degrees of freedom of modulating the pentagrid into a commensurate one; further generalizations remain. First, we can alternatively fix the grids 1 and 3 instead of 1 and 2. The difference between these two choices affects the shape of the unit cell of the modulated pentagrid and its dual lattice. The unit cell is a parallelogram with angle $2\pi/5$ when grids 1 and 2 are fixed, while it is a parallelogram with an angle $\pi/5$ for grids 1 and 3. Second, there remains the degree of freedom of modulating the two fixed grids. We may change the angle and the spacings of the two grids. With these modulations, we can generate a wider range of periodic approximations of the original PL.

3. Periodic Penrose lattices and semiperiodic Penrose lattices

Following the procedures explained above, we generate two special sequences of systematic approximations of the PL (Ref. 29) for use in numerical computations—the periodic Penrose lattices (PPL) and the semiperiodic Penrose lattices (SPPL). The PPL will be used mainly for the study of electronic structure, while the SPPL for the study of length dependence of the conductance.

The periodic approximations of the lattice are determined by the approximants of the golden ratio τ. The optimal approximants are, as is well known, the ratios of successive Fibonacci numbers $\tau\sim\tau_n\equiv F_{n+1}/F_n$. Here, $\{F_n\}$ is defined by the recursion relation $F_{n+1}=F_n+F_{n-1}$ with the initial values $F_1=1$, $F_2=2$, and in the explicit form $F_n=[\tau^{n+1}-(-\tau)^{-(n+1)}]/\sqrt{5}$. As n increases, the approximant approaches the golden ratio rapidly while oscillating around it: $\tau-\tau_n\sim(-1)^n\sqrt{5}\tau^{-2n-2}$. Thus the golden ratio can be systematically approximated by the sequence $\{\tau_n\}=\{2,\frac{3}{2},\frac{5}{3},\frac{8}{5},\frac{13}{8},\frac{21}{13},\ldots\}$.

First, we generate a sequence of the periodic approximations by substituting τ_n for all r's and s's in Eq. (A5) fixing grids 1 and 2. This choice provides periodic lattices with unit cells in the shape of a thick Penrose rhombus. We shall call them the *periodic Penrose lattices* hereafter. Some examples of the unit cells of the PPL are shown in Fig. 6. The PPL have the following properties: (1) the periodic boundary condition can be imposed on the unit cell in both of the two directions; (2) the unit cell has a fatter shape than selected in fixing grids 1 and 3; (3) there are no extra modulations for the pentagrid. Property (2) means that the number of sites on the boundary is smaller and the boundary effect is accordingly less critical in numerical computations. Property (3) means modulation of the lattice is the least possible. A remarkable fact is that the number of defects, i.e., vertex edges where the Penrose matching rule is violated, can be reduced to two per unit cell, irrespective of unit-cell size.[29] This means that the PPL are the optimal approximations.

For the study of length dependence of conductance, another type of approximation is more appropriate: i.e., the lattices quasiperiodic in the direction in which we extend the lattice. To this end, we must modulate the pentagrid so that it is periodic only in one direction while retaining quasiperiodicity in the other direction. This requirement is fulfilled by the modulation (A5) in which only r_3 and r_4 are substituted by τ_n, and s_4 and s_5 remain τ. The corresponding dual lattices are consequently periodic in one direction but quasiperiodic in the other direction, and we shall call them the *semiperiodic Penrose lattices* hereafter. In Fig. 7, we show a part of a SPPL for $\tau_n=\frac{5}{3}$. Defects in SPPL are not analyzed in detail yet, but the defect density decreases as the approximation improves.

Analyzing the structure of the PPL more quantitative-

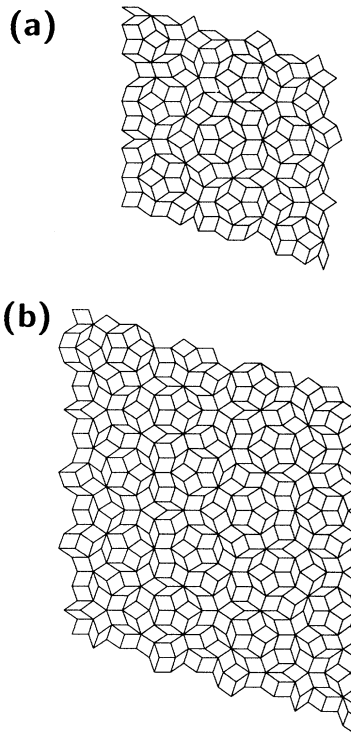

FIG. 6. Unit cells of the periodic Penrose lattices. (a) $\tau_n=\frac{5}{3}$, $M=16$, $N=199$; (b) $\tau_n=\frac{8}{5}$, $M=26$, $N=521$.

ly: for a PPL, the grid vectors are explicitly given by

$$\begin{aligned}
&\tilde{\mathbf{e}}_1=(1,0),\quad \tilde{\mathbf{e}}_2=(\cos\phi,\sin\phi)\ ,\\
&\tilde{\mathbf{e}}_3=\left[\frac{1}{\tau_n}\cos\phi-1,\frac{1}{\tau_n}\sin\phi\right]\ ,\\
&\tilde{\mathbf{e}}_4=-\frac{1}{\tau_n}(\cos\phi+1,\sin\phi)\ ,\\
&\tilde{\mathbf{e}}_5=\left[\frac{1}{\tau_n}-\cos\phi,-\sin\phi\right]\ ,
\end{aligned}\tag{A6}$$

where, again, an approximant of the golden ratio is set to $\tau_n=F_{n+1}/F_n$ and $\phi=2\pi/5$. Let us count the number of rhombuses in the unit cell. This is given by the number of intersections of the grids in the unit cell of the modulated pentagrid, and the number of intersections N_{ij} for each grid pair (i,j) is determined by the ratio of the area of the pentagrid unit cell to the area of the smallest parallelogram made by the specified grid pair:

$$N_{ij}=F_{n+1}^2 a\,|\tilde{\mathbf{e}}_i\times\tilde{\mathbf{e}}_j|\ .\tag{A7}$$

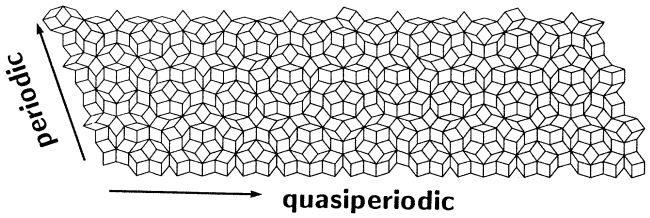

FIG. 7. A part of the semiperiodic Penrose lattice generated by $\tau_n=\frac{5}{3}$. $M=16$.

Now it is a straightforward calculation to obtain the numbers of fat and thin rhombuses and the total number:

$$N^{\text{fat}}=3F_{n+1}^2+2F_nF_{n+2}=F_{2n+4}+F_{2n+2}\ ,\tag{A8a}$$

$$N^{\text{thin}}=4F_nF_{n+1}+F_{n-1}F_{n+2}=F_{2n+3}+F_{2n+1}\ ,\tag{A8b}$$

$$N=N^{\text{fat}}+N^{\text{thin}}=F_{2n+5}+F_{2n+3}\ ,\tag{A8c}$$

where the addition formula $F_{n+m}=F_nF_m+F_{n-1}F_{m-1}$ is used for the derivation.

Next, let us define the width of the unit cell. Consider a unit cell of a PPL, then we notice that the grid which we fixed in the generation procedure consists of quasiperiodically spaced rhombus arrays (called segments), and the number of rhombuses in each segment is the same. Define the *width* of the unit cell by the number of rhombuses; this is given by

$$M=\frac{1}{F_{n+1}}(N_{12}+N_{13}+N_{14}+N_{15})=2F_{n+2}\ .\tag{A9}$$

For example, for the PPL generated by approximants $\tau_n=\frac{3}{2},\frac{5}{3},\frac{8}{5},\frac{13}{8},\frac{21}{13}$, the rhombus numbers are $N=76,199,521,1364,3571$, and the widths are $M=10,16,26,42,68$, respectively.

Analysis of the SPPL can be done similarly, but note that only r_3 and r_4 are approximated into τ_n in this case, which means that the modified pentagrid has only one translation vector. We can easily count the number of intersections of the translation vector and the other grids $j=2,\ldots,5$, and the result is

$$M_2=M_5=F_{n+1},\quad M_3=M_4=\frac{F_{n+1}}{\tau_n}=F_n\ .\tag{A10}$$

The SPPL can be regarded as a periodic stack of strips of infinite length. As in the PPL case, define the strip width by the number of rhombuses that are located on the segment corresponding to the translation vector, then

$$\begin{aligned}
M&=M_2+M_3+M_4+M_5\\
&=2(F_n+F_{n+1})=2F_{n+2}\ ,
\end{aligned}\tag{A11}$$

and this result coincides with the value for the PPL generated by the same τ_n.

[1]D. Shechtman, I. Blech, D. Gratias, and J. W. Cahn, Phys. Rev. Lett. **53**, 1951 (1984).
[2]D. Levine and P. J. Steinhardt, Phys. Rev. Lett. **53**, 2477 (1984).
[3]See Ref. 2 and P. J. Steinhardt and S. Ostlund, *The Physics of Quasicrystals* (World Scientific, Singapore, 1987).
[4]For example, S. J. Poon, A. J. Drehman, and K. R. Lawless, Phys. Rev. Lett. **55**, 2324 (1985).
[5]L. Bendersky, Phys. Rev. Lett. **55**, 1461 (1985).
[6]P. Sainfort and B. Dubost, J. Phys. (Paris) Suppl. **47**, C3-321 (1986); P. A. Tsai, A. Inoue, and T. Masumoto, Jpn. J. Appl. Phys. **26**, L1505 (1987).

[7]For a review, see P. A. Lee and T. V. Ramakrishnan, Rev. Mod. Phys. **57**, 287 (1985).

[8]M. Kohmoto, L. P. Kadanoff, and C. Tang, Phys. Rev. Lett. **50**, 1870 (1983); S. Ostlund, R. Pandit, D. Rand, H. J. Schellnhuber, and E. D. Siggia, *ibid.* **50**, 1873 (1983).

[9]S. Kotani, Publ. Res. Inst. Math. Sci. (Kyoto), No. 692 (1989); A. Sütö, J. Stat. Phys. **56**, 525 (1989).

[10]M. Kohmoto, B. Sutherland, and C. Tang, Phys. Rev. B **35**, 1020 (1987).

[11]Some 1D quasiperiodic models have extended eigenstates at particular energies. See, for example, V. Kumar and G. Ananthakrishna, Phys. Rev. Lett. **59**, 1476 (1987); T. Dotera (private communication); V. Kumar, J. Phys. Condens. Matter **2**, 1349 (1990). The last example is a special case of 1D disordered systems where the on-site energies and the transfer integrals are correlated. It is shown by Dunlap *et al.* that in such systems $\sqrt{N}$ of the eigenstates become extended; D. H. Dunlap, H-L. Wu, and P. W. Phillips, Phys. Rev. Lett. **65**, 88 (1990). But extended states in these models are exceptional, since the measure of such energies is zero.

[12]See Ref. 10, and T. Fujiwara, M. Kohmoto, and T. Tokihiro, Phys. Rev. B **40**, 7413 (1989).

[13]S. Aubry and G. André, Ann. Israel Phys. Soc. **3**, 133 (1980); S. Ostlund and R. Pandit, Phys. Rev. B **29**, 1394 (1984).

[14]The frustration effect was also pointed out for structural disordered materials by M. H. Cohen, J. Singh, and F. Yonezawa, Solid State Commun. **36**, 923 (1980).

[15]R. Penrose, Bull. Inst. Math. Appl. **10**, 266 (1974).

[16]M. Gardner, Sci. Am. **236** (1), 110 (1977).

[17]K. Semba, Master's thesis, Tokyo University, 1985; T. C. Choy, Phys. Rev. Lett. **55**, 2915 (1985); T. Odagaki and D. Nguyen, Phys. Rev. B **33**, 2184 (1986).

[18]K. Semba in Ref. 17; K. Semba and T. Ninomiya (private communication); T. Fujiwara, M. Arai, T. Tokihiro, and M. Kohmoto, Phys. Rev. B **37**, 2797 (1988).

[19]M. Kohmoto and B. Sutherland, Phys. Rev. Lett. **56**, 2740 (1986).

[20]M. Arai, T. Tokihiro, T. Fujiwara, and M. Kohmoto, Phys. Rev. B **38**, 1621 (1988).

[21]However, they are stable for some special perturbations. See Ref. 19 and T. Hatakeyama and H. Kamimura, Solid State Commun. **62**, 79 (1987).

[22]B. Sutherland, Phys. Rev. B **34**, 3904 (1986); T. Tokihiro, T. Fujiwara, and M. Arai, *ibid.* **38**, 5981 (1988).

[23]H. Tsunetsugu, T. Fujiwara, K. Ueda, and T. Tokihiro, J. Phys. Soc. Jpn. **55**, 1420 (1986).

[24]H. Tsunetsugu and K. Ueda, Phys. Rev. B **38**, 10 109 (1988).

[25]Here we do not consider the models which include long-range electron transfers since, in those models, some modifications are necessary for the argument.

[26]E. J. Dinaburg and Ya. G. Sinai, Func. Anal. Appl. **9**, 279 (1975); Ya. G. Sinai, J. Stat. Phys. **46**, 861 (1987).

[27]An attempt was made on higher-dimensional models under certain restrictions: T. Ninomiya, J. Non-Cryst. Solids **117/118**, 777 (1990).

[28]V. Elser and C. L. Henley, Phys. Rev. Lett. **55**, 2883 (1985).

[29]For the 2D case, see O. Entin-Wohlman, M. Kléman, and A. Pavlovitch, J. Phys. (Paris) **49**, 587 (1988).

[30]An anomalous level spacing distribution was observed for the FC: M. Fujita and K. Machida, J. Phys. Soc. Jpn. **56**, 1470 (1987).

[31]S. A. Molčanov, Commun. Math. Phys. **78**, 429 (1981).

[32]K. Ueda and H. Tsunetsugu, Phys. Rev. Lett. **58**, 1272 (1987).

[33]P. Dean, Proc. R. Soc. London **260**, 263 (1961).

[34]By varying p, the $2p$ norm provides information equivalent to that derived from the multifractal analysis. See Tokihiro *et al.* in Ref. 22.

[35]N. G. de Bruijn, Indag. Math. Proc. Ser. A **89**, 39 (1981); **89**, 53 (1981).

[36]F. Gähler and J. Rhyner, J. Phys. A **19**, 267 (1986).